INTERNATIONAL JOURNAL FOR NUMERICAL METHODS IN FLUIDS
Int. J. Numer. Meth. Fluids 2001; **35**: 743–761

A fictitious domain/mortar element method for fluid–structure interaction

Frank P. T. Baaijens*,[1]

Faculty of Mechanical Engineering and Faculty of Biomedical Engineering, Eindhoven University of Technology, Eindhoven, Netherlands

SUMMARY

A new method for the computational analysis of fluid–structure interaction of a Newtonian fluid with slender bodies is developed. It combines ideas of the fictitious domain and the mortar element method by imposing continuity of the velocity field along an interface by means of Lagrange multipliers. The key advantage of the method is that it circumvents the need for complicated mesh movement strategies common in arbitrary Lagrangian–Eulerian (ALE) methods, usually used for this purpose. Copyright © 2001 John Wiley & Sons, Ltd.

KEY WORDS: fluid–structure interaction; Lagrange multipliers; mortar element method

1. INTRODUCTION

There exist many examples where the motion of thin-walled, leaflet-like structure is driven by the motion of a fluid. A typical example in biomechanics is the opening and closing behaviour of aortic heart-valves, which is a delicate interaction between blood flow and geometrical and stiffness properties of the heart-valve leaflets, see de Hart *et al.* [1] and Cacciola *et al.* [2].

In modelling fluid–structure interaction, the fluid phase is most conveniently described with respect to a Eulerian reference frame, while a Lagrangian formulation is more appropriate for the solid phase. However, these formulations are incompatible. The arbitrary Lagrangian–Eulerian (ALE) formulation first proposed by Donea [3], effectively combines these two formulations and is often applied for fluid–structure interaction simulations. The ALE formulation requires a continuous adaptation of the mesh without modification of the mesh topology. Due to the finite deformation of a thin leaflet within the computational domain it is generally difficult to adapt the mesh in such a way that a proper mesh quality is maintained without changing the mesh topology. An example of this will be given in Section 6.1.

* Correspondence to: Faculty of Mechanical Engineering and Faculty of Biomedical Engineering, Eindhoven University of Technology, PO Box 513, 5600 MB Eindhoven, Netherlands.
[1] E-mail: baaijens@wfw.wtb.tue.nl

Received May 1999
Revised May 2000

Alternatively, remeshing can be performed using a Lagrangian formulation or in conjunction with an ALE formulation, where remeshing is only performed if the mesh quality has degenerated too much. The change in mesh topology during remeshing requires the use of interpolation techniques to recover history variables on the newly generated mesh. This not only introduces artificial diffusivity, but it is also difficult and/or time-consuming to perform with sufficient robustness and accuracy for three-dimensional problems. To resolve this problem, a new fictitious domain/mortar element (FD/ME) method is proposed, where the fluid is described using a fixed mesh in an Eulerian setting and a Lagrangian formulation for the solid. It is based on a combination the fictitious domain method, as described by Glowinski *et al.* [4], and the mortar element method, developed by, among others, Bernardi *et al.* [5] and Maday *et al.* [6].

The fictitious domain (FD) method is based on the imposition of velocity constraints associated with *rigid* internal boundaries by means of Lagrange multipliers. It has similarities with the so-called immersed boundary technique of Peskin and McQueen [7], in which at a number of control points (at the intersection of fluid and solid), tension forces are imposed pointwise and distributed to neighbouring nodes. A variant of this method, the immersed interface method, has been proposed in Reference [8]. More recently, Bertrand *et al.* [9] have introduced a special variant of the FD method by using point collocation, circumventing the judicious choice of base functions of the Lagrange multiplier.

The mortar element (ME) method allows coupling of domains with dissimilar element distributions or interpolation order using Lagrange multipliers as outlined by Schwab [10]. The edges of these domains must have the same geometrical position, in other words element edges should overlap and the intersection of the domains should be empty.

The FD/ME proposed in this work is based on a Lagrange multiplier formulation and on concepts and interpolation schemes of the ME method but without the requirement that element edges should overlap. In this sense, it incorporates ideas of the FD method. The current implementation is limited to two-dimensional problems, but it clearly demonstrates the capabilities of the computational scheme, which is the objective of this paper.

First, the problem definition in conjunction with the governing equations are given. The fluid is modelled using the Navier–Stokes equations in a Eulerian setting and the solid is described with a neo-Hookean material model in an updated Lagrange formulation. Then the Lagrange multiplier formulation is outlined based on the weak formulation of both the fluid and solid domain. Next, the FD/ME method is validated for Stokes flow conditions by comparison with an updated mesh (ALE-like) formulation. Subsequently, the capabilities are demonstrated for the two-dimensional motion of a flexible leaflet in a periodic flow. This example mimics the motion of heart-valve leaflets in a two-dimensional setting.

2. PROBLEM DEFINITION AND GOVERNING EQUATIONS

The objective is to analyse the motion of a slender body (e.g. leaflet) inside a Newtonian fluid. In this work, the typical dimension of the solid body in the longitudinal direction is chosen large compared with the orthogonal direction (thickness). In fact, as far as fluid–structure interaction is concerned, the thickness of the solid body may be neglected. Although a

volumetric representation of the solid is chosen in this work, shell (three-dimensional) or beam (two-dimensional) theories could also be used to describe the mechanical behaviour of the solid body.

2.1. Fluid domain

The fluid is assumed to be isothermal and incompressible and the governing equations within the fluid domain Ω_f, in absence of body forces, are given by

$$\rho \frac{\partial \vec{u}}{\partial t} + \rho \vec{u} \cdot \vec{\nabla} \vec{u} = \vec{\nabla} \cdot (-p\boldsymbol{I} + \boldsymbol{\tau}_f) \tag{1}$$

$$\vec{\nabla} \cdot \vec{u} = 0 \tag{2}$$

where ρ denotes the density, t the time, $\vec{u}$ the velocity, p the pressure, $\boldsymbol{\tau}_f$ the extra stress tensor and $\vec{\nabla}$ the gradient operator with respect to the current configuration.

Clearly, the above set of equations must be complemented with appropriate natural and Dirichlet boundary conditions. For the purpose of this work it is sufficient to consider Dirichlet boundary conditions only.

The fluid is assumed to be Newtonian, hence the extra stress tensor is given by

$$\boldsymbol{\tau}_f = 2\eta \boldsymbol{D} \tag{3}$$

where η denotes the viscosity of the fluid and $\boldsymbol{D}$ denotes the rate of deformation tensor $\boldsymbol{D} = \frac{1}{2}(\vec{\nabla}\vec{u} + (\vec{\nabla}\vec{u})^T)$. Substitution of this constitutive model into Equation (1) yields the well-known Navier–Stokes equation

$$\rho \frac{\partial \vec{u}}{\partial t} + \rho \vec{u} \cdot \vec{\nabla} \vec{u} = -\vec{\nabla} p + \vec{\nabla} \cdot 2\eta \boldsymbol{D} \tag{4}$$

Scaling spatial co-ordinates with a characteristic length H (e.g. channel height), velocities with a characteristic velocity U (e.g. mean velocity) and time with a characteristic time τ (e.g. period), the dimensionless form of the Navier–Stokes equation is given by

$$St \frac{\partial \vec{u}}{\partial t} + \vec{u} \cdot \vec{\nabla} \vec{u} = -\vec{\nabla} p + \frac{1}{Re} 2\vec{\nabla} \cdot \boldsymbol{D} \tag{5}$$

where the Strouhal number St and the Reynolds number Re are defined as

$$St = \frac{H}{\tau U}, \qquad Re = \frac{\rho U H}{\eta} \tag{6}$$

2.2. Solid domain

In the absence of inertia terms, the momentum equation for the solid domain Ω_s reduces to

$$\vec{\nabla}\cdot(-p\boldsymbol{I}+\boldsymbol{\tau}_s)=\vec{0} \tag{7}$$

while the incompressibility condition is conveniently expressed as

$$\det(\boldsymbol{F})=1 \tag{8}$$

where $\boldsymbol{F}$ denotes the deformation tensor, defined as $\boldsymbol{F}=(\vec{\nabla}_0\vec{x})^T$, with $\vec{\nabla}_0$ the gradient operator with respect to the reference configuration.

The solid is assumed to obey a neo-Hookean material law, hence

$$\boldsymbol{\tau}_s=G(\boldsymbol{B}-\boldsymbol{I}) \tag{9}$$

where G is the shear modulus and $\boldsymbol{B}$ the Finger or left Cauchy–Green strain tensor, defined as $\boldsymbol{B}=\boldsymbol{F}\cdot\boldsymbol{F}^T$. Expression (9) has been chosen such that the extra stress in the solid vanishes if $\boldsymbol{F}=\boldsymbol{I}$.

3. WEAK FORMULATION

Assuming absence of externally applied surface loads, the weak form of the momentum and continuity equation (1) and (2) are given by

$$\left(\vec{v},\ \rho\frac{\partial\vec{u}}{\partial t}+\rho\vec{u}\cdot\vec{\nabla}\vec{u}\right)+(\boldsymbol{D}_v,2\eta\boldsymbol{D})-(p,\vec{\nabla}\cdot\vec{v})=0 \tag{10}$$

$$(q,\vec{\nabla}\cdot\vec{u})=0 \tag{11}$$

where $(\,.\,,.\,)$ denotes the appropriate inner product on the fluid domain Ω_f and $\boldsymbol{D}_v=\frac{1}{2}(\vec{\nabla}\vec{v}+(\vec{\nabla}\vec{v})^T)$. These must hold for all admissible weighting functions $\vec{v}$ and q. Temporal discretization is achieved using an implicit backward-Euler scheme. Consider the time interval $t_n\rightarrow t_{n+1}$, such that $\Delta t=t_{n+1}-t_n$, then

$$\frac{\partial\vec{u}}{\partial t}\approx\frac{\vec{u}_{n+1}-\vec{u}_n}{\Delta t} \tag{12}$$

This choice leads to a scheme that is first-order accurate in time only. This is sufficient to demonstrate the characteristics of the proposed method, but for many applications higher-order approximations are recommended. Consequently, Equation (10) is rewritten, omitting the subscript $n+1$, as

$$\left(\vec{v},\ \rho\frac{\vec{u}-\vec{u}_n}{\Delta t}+\rho\vec{u}\cdot\vec{\nabla}\vec{u}\right)+(\boldsymbol{D}_v,\ 2\eta\boldsymbol{D})-(p,\ \vec{\nabla}\cdot\vec{v})=0 \tag{13}$$

For the solid phase an updated Lagrangian formulation is chosen. Let $\boldsymbol{F}_n$ denote the deformation from the initial state to the state at $t=t_n$, and $\boldsymbol{F}_{n+1}$ the deformation tensor from $t=t_n$ to $t=t_{n+1}$, then

$$\boldsymbol{F}=\boldsymbol{F}_{n+1}\cdot\boldsymbol{F}_n \tag{14}$$

For notational convenience we shall, as before, omit the subscript $n+1$; hence, in the sequel $\boldsymbol{F}$ refers to the deformation tensor from the previous state to the current state. Then, the extra stress tensor of the solid at the current time t can be written as

$$\boldsymbol{\tau}_s=\boldsymbol{F}\cdot\boldsymbol{\tau}_n\cdot\boldsymbol{F}^T+G(\boldsymbol{F}\cdot\boldsymbol{F}^T-\boldsymbol{I}) \tag{15}$$

where $\boldsymbol{\tau}_n$ denotes the extra stress at time $t=t_n$ and $\boldsymbol{I}$ the second-order unit tensor. Consequently, the weak form within an updated Lagrangian framework of the solid can be written as

$$[(\nabla\vec{v})^T,\ \boldsymbol{F}\cdot\boldsymbol{\tau}_n\cdot\boldsymbol{F}^T+G(\boldsymbol{F}\cdot\boldsymbol{F}^T-\boldsymbol{I})]-[p,\ \vec{\nabla}\cdot\vec{v}]=0 \tag{16}$$

$$[q,\ \det(\boldsymbol{F})-1]=0 \tag{17}$$

where $[\,.\,,\,.\,]$ denotes the appropriate inner product on the solid domain Ω_s.

Notice that there is a distinct difference between Equation (10) and equation (16): in the weak form of the momentum equation of the fluid the domain is known and fixed in space, unless specified otherwise, while the position of the solid domain is *a priori* unknown. As a consequence, for instance, the gradient operator in Equation (16) depends on the solution, while the gradient operator in Equation (10) is independent of the velocity field $\vec{u}$. This situation changes whenever the computational domain of the fluid is adapted to the computed velocity field, for instance, to follow the motion of the slender body. For the time being, however, the fluid domain is assumed fixed in space.

In the Lagrangian formulation it is customary to chose the displacement field $\vec{d}$ as the unknown. The displacement during a time step $t_n\to t_{n+1}$ follows from

$$\vec{d}=\vec{x}_{n+1}-\vec{x}_n \tag{18}$$

where $\vec{x}_n$, $\vec{x}_{n+1}$ denote the position of a material point at time $t=t_n$ and $t=t_{n+1}$ respectively. The velocity during the time interval $t_n\to t_{n+1}$ is related to the displacement by the following first-order approximation:

$$\vec{u}=\frac{\vec{d}}{\Delta t} \tag{19}$$

4. MORTAR ELEMENT METHOD

Coupling of the fluid and solid domain is straightforward if equal-order discretization of the fluid and solid domain is used and nodes and element boundaries are coincident along the relevant boundary. In this case, the fluid mesh must be updated continuously to accommodate for the motion of the solid domain using the ALE formulation. In this section a formulation is proposed that circumvents the need to update the fluid mesh.

For non-equal and/or non-conforming discretizations, but still coincident boundaries, the so-called mortar element method has been developed. Applied to fluid–structure interaction, coupling between the fluid and solid phase is achieved by using a Lagrange multiplier to weakly enforce the constraint $\vec{u}_s - \vec{u}_f = \vec{0}$ along the interface boundary Γ. This procedure is outlined for the infinitesimal strain limit for linear elastic bodies in Appendix A, and may be generalized to

$$\left(\vec{v}_f,\ \rho\frac{\partial \vec{u}_f}{\partial t} + \rho\vec{u}_f\cdot\vec{\nabla}\vec{u}_f\right) + (\boldsymbol{D}_v,\ 2\eta\boldsymbol{D}) - (p,\ \vec{\nabla}\cdot\vec{v}_f) - \int_\Gamma \vec{\gamma}\cdot\vec{v}_f\,\mathrm{d}\Gamma = 0 \tag{20}$$

$$(q,\ \vec{\nabla}\cdot\vec{u}_f) = 0 \tag{21}$$

$$[(\nabla\vec{v}_s)^T,\ \boldsymbol{F}\cdot\boldsymbol{\tau}_n\cdot\boldsymbol{F}^T + G(\boldsymbol{F}\cdot\boldsymbol{F}^T - \boldsymbol{I})] - [p,\ \vec{\nabla}\cdot\vec{v}_s] + \int_\Gamma \vec{\gamma}\cdot\vec{v}_s\,\mathrm{d}\Gamma = 0 \tag{22}$$

$$[q,\ \det(\boldsymbol{F}) - 1] = 0 \tag{23}$$

$$\int_\Gamma \vec{\lambda}\cdot(\vec{u}_s - \vec{u}_f)\,\mathrm{d}\Gamma = 0 \tag{24}$$

The subscripts 'f' and 's' have been introduced to differentiate between the fluid and solid domain variables respectively. The Lagrange multiplier is denoted by $\vec{\gamma}$, with $\vec{\lambda}$ the associated weight function, and may be interpreted as the surface force exerted on the fluid and solid along the interface Γ to maintain the coupling between solid and fluid.

In fluid–structure interaction problems, the location of the interface boundary Γ depends on the solution $\vec{u}_s$. Consequently, to maintain coincident fluid and solid boundaries the fluid domain needs to be updated accordingly. This can effectively be achieved using the ALE method or by using remeshing techniques. However, for arbitrary finite deformations of the solid it is difficult to robustly maintain mesh quality, in particular for three-dimensional problems. Two-dimensional examples of this will be given later on.

To circumvent the need to update the mesh of the fluid domain a new approach is proposed. It combines features of the so-called fictitious domain method, developed by Glowinski *et al.* [4], and the ME method [6]. Consequently, we shall label this formulation the FD/ME approach. It is governed by Equations (20)–(24).

The novelty of the current approach is that the surface Γ does not necessarily have to be aligned with element boundaries of the fluid domain. In fact, Γ does not necessarily have to coincide with a boundary of the solid domain either, although it is convenient. A typical

example is given in Figure 3, where the interface is aligned with one side of the solid body. Clearly, the interface Γ intersects the fluid domain in an arbitrary way. The alignment with only one side of the solid body appears to be particularly suitable for problems with slender solid bodies of which the thickness may be assumed negligible as far as the interaction with the fluid flow is concerned. Otherwise, the complete boundary of the solid needs to be chosen as the interface Γ. In that case, however, care should be taken at non-zero Strouhal and Reynolds numbers, since the fluid enclosed by Γ must be accelerated as well.

The resulting set of coupled equations (20)–(24) is non-linear and needs to be solved iteratively. Each of the couples (20)–(21) and (22)-(23) is linearized using Newton's method. The coupling through Equation (24) is enforced at each Newton iteration using the most recently computed location of the boundary Γ. The location of the interface Γ is not known *a priori* and linearization of this aspect is difficult. Since the repositioning of the interface location is not taken into account during the linearization process, the quadratic convergence rate of the Newton scheme is not obtained but the chosen strategy has proven to give satisfactory results.

At each integration point used to compute the integrals related to the Lagrange multipliers, the isoparametric co-ordinates of the solid are obtained trivially since the spatial discretization coincides with the edge of the solid domain. However, the velocity at the associated fluid particle must be computed as well. This requires identification of the element and the isoparametric co-ordinates of the fluid particle coincident with the spatial location of the integration point. Once these co-ordinates are known, the shape functions of the velocity field are used to express the fluid velocity at the integration point in terms of the nodal velocities of the fluid domain.

5. DISCRETIZATION

It is well established that the mixed velocity–pressure formulations defined above need to satisfy the so-called inf–sup condition. A variety of discretization schemes is available that satisfy this conditions. Here the Crouzeix–Raviart family has been used, in the sense that a bi-quadratic interpolation for the velocity is used and a linear discontinuous interpolation for the pressure. The same discretization is chosen for the displacement–pressure combination of the solid phase.

In combination with the constraint equation (24) coupling fluid to solid velocities with an arbitrary location of the boundary Γ, a discontinuous interpolation of the pressure appears to be mandatory. A continuous interpolation of the pressure, as in the Taylor–Hood family, produced unsatisfactory results. This can easily be understood by considering a domain with an internal line boundary, as depicted in Figure 1(a) denoted by the boundary Γ_5. If velocities are set to zero along this internal boundary, the pressure will be discontinuous across this boundary. Hence, the use of a continuously interpolated pressure leads to erroneous results. Although in the FD/ME method the interface Γ is not necessarily aligned with element boundaries of the fluid domain, a discontinuity in the pressure field may be expected.

The failure of the Taylor–Hood element in the case of an internal boundary is illustrated next. In problem A, outlined in Figure 1(a), the fluid domain is enclosed by the boundaries

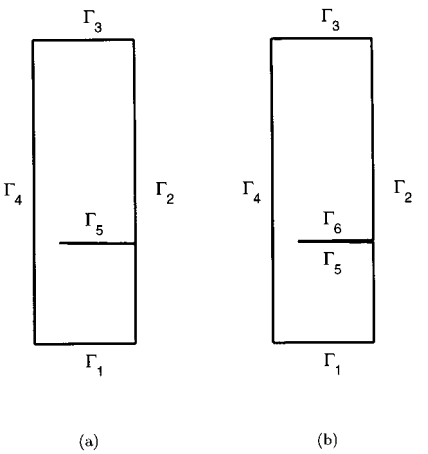

Figure 1. (a) Problem A with an internal interface Γ_5, and (b) problem B with a discontinuous internal boundary characterized by the boundaries Γ_5 and Γ_6.

Γ_1–Γ_4. Along Γ_1 a fully developed inflow velocity profile is prescribed, while along Γ_2 and Γ_5 no-slip boundary conditions are imposed. Along Γ_3 the velocity in the horizontal direction is set to zero to represent a symmetry condition. Along the outflow direction the horizontal velocity is set to zero as well. Notice that in this problem the elements on either side of the internal boundary, Γ_5, share the same node on this part of the boundary. This implies that if the pressure is interpolated continuously, as in the Taylor–Hood element, it is continuous across the boundary Γ_5. To allow for a discontinuous interpolation of the pressure across the internal boundary in case of the Taylor–Hood element, a slight modification is made, labelled problem B, as outline in Figure 1(b). In this case a very small wedge is created by including boundary Γ_6, such that elements on either sides of the internal boundary have different nodes. This clearly allows for a discontinuous interpolation of the pressure field across the internal boundary. The resulting streamlines at a Reynolds number of 10 are depicted in Figure 2. Figure 2(a) displays the streamlines for the Crouzeix–Raviart element for problem A. This is clearly significantly different form the incorrect results of the Taylor–Hood element, as depicted in Figure 2(b). Using a discontinuous internal boundary, problem B, the Taylor–Hood produces the correct result, as shown in Figure 2(c).

The discretization of the Lagrange multiplier $\vec{\gamma}$, and hence also $\vec{\lambda}$, has been chosen linear, discontinuous and spatially coincident with element boundaries of the solid domain: along each element boundary of solid domain that coincides with Γ a piecewise linear discontinuous interpolation of $\vec{\lambda}$ is chosen. More generally, the interpolation order of the Lagrange multiplier field is chosen one order lower than the interpolation order of the velocity field. The choice of a discontinuous quadratic interpolation of the Lagrange multiplier would lead to an overconstrained set of equations. This can be understood by investigating the case were Γ consists of two neighbouring element edges. Suppose that a quadratic interpolation of the displacement field is chosen as well as a discontinuous quadratic interpolation of the Lagrange multiplier.

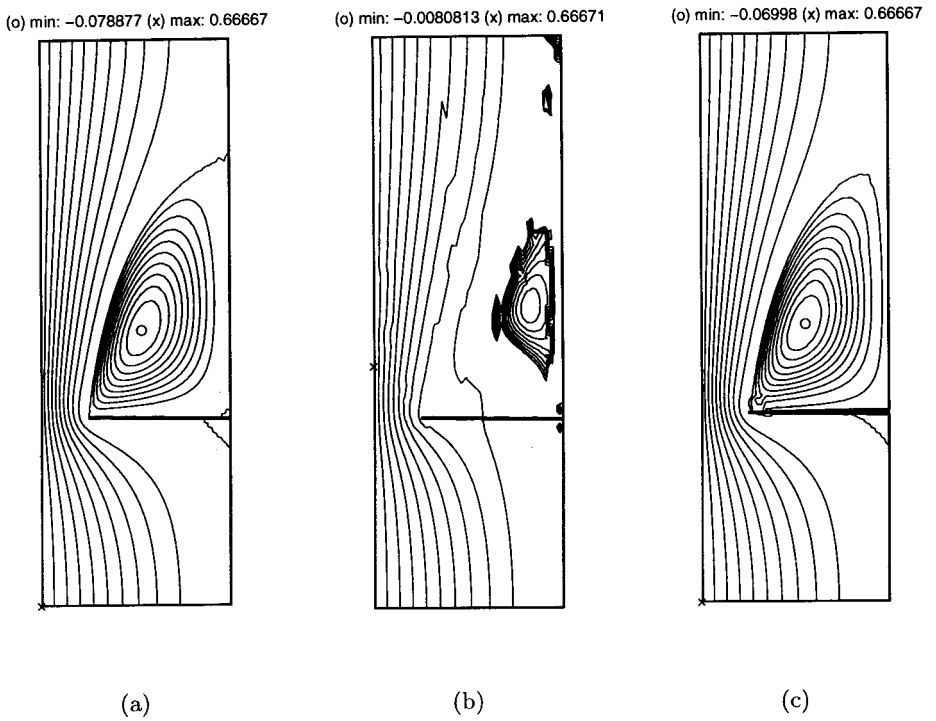

Figure 2. Streamlines at $Re = 10$ for (a) Crouzeix–Raviart element, (b) Taylor–Hood element and (c) Taylor–Hood element but for the problem with a discontinuous internal boundary.

Then, the Lagrange multiplier generates 12 constraints, while the boundary Γ (having five nodes) has only ten degrees of freedom. The above choice has been found to give optimal results and is consistent with results from 'regular' ME applications. The integral along Γ, as in Equations (20), (22) and (24), is computed by means of a Gaussian integration rule. Given the lower-order interpolation of the Lagrange multiplier compared with the velocity interpolation, Gauss–Lobatto integration is not feasible. Furthermore, aligning the interface Γ with element boundaries of the solid domain as described above, spatial resolution of the solid domain preferably needs to be higher than that of the fluid domain. An example of this is given in Figure 3.

6. VALIDATION AND APPLICATION

The examined problem is illustrated in Figure 4(a) in conjunction with the mesh for both the fluid and the solid body. The fluid domain in enclosed by the boundaries Γ_1–Γ_4. In Figure 4(b) a close-up of the mesh near the attachment of the solid to boundary Γ_2 is shown. The solid

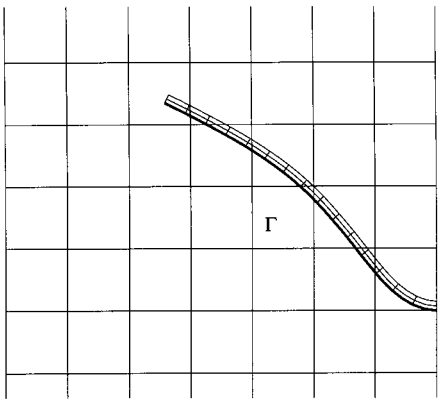

Figure 3. Example of interface (Γ) location, represented by the thick line.

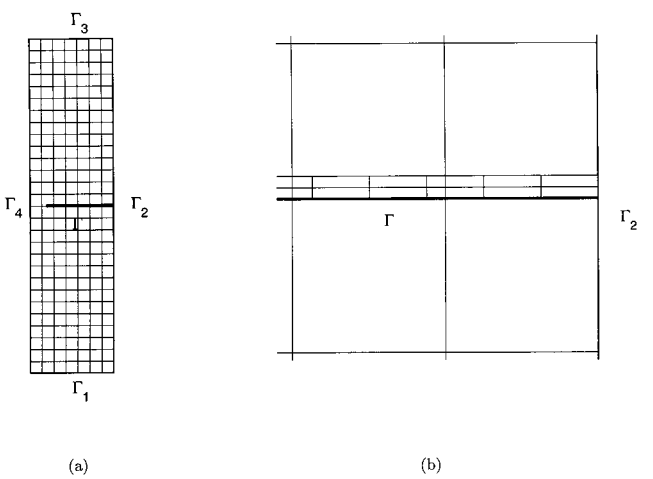

Figure 4. (a) Geometry and mesh of the test problem, (b) close-up near the attachment point of the beam.

may be interpreted as a thin beam that is fixed at the right end, and is modelled using neo-Hookean material behaviour. Connection between fluid and solid is established along the interface boundary Γ only. In the initial configuration, Γ is aligned with element boundaries of the fluid as can be seen in Figure 4(b).

Along Γ_2 all velocities are suppressed, while along Γ_4 symmetry conditions are imposed, meaning that velocities in the horizontal direction are suppressed. The velocity components at Γ_1 and Γ_3 are coupled by means of periodic boundary conditions.

Along Γ_1 the flow rate is prescribed according to

$$Q = U \sin(2\pi t), \quad U = 10 \tag{25}$$

meaning that the period $T = 1$. In terms of velocities, the flow rate can be written as

$$Q = -\int_{\Gamma_1} \vec{u} \cdot \vec{n} \, d\Gamma \tag{26}$$

where $\vec{n}$ is the unit outward normal to Γ_1. Using the shape functions of the velocity components and performing a numerical integration, these equations can be transformed into an algebraic equation, resulting in a linear equation coupling the velocity degrees of freedom along the interface boundary. This equation is imposed by means of an additional Lagrange multiplier. In conjunction with the periodicity of the flow velocity, this yields a unique velocity distribution along the inflow and outflow boundary.

If $H = 1$ represents the horizontal dimension of the flow domain, then the height equals $4H$, the thickness of the beam is $0.0212H$ and the length of the beam is $0.8H$.

The viscosity $\eta = 10$, the modulus G is chosen to be 10^7. The density is either set to zero in the limit of Stokes flow, or is chosen as 10^2. Consequently, for non-Stokes flow conditions the Strouhal and Reynolds number are

$$St = 0.1, \qquad Re = 100 \tag{27}$$

6.1. Stokes flow

To investigate the performance of the proposed scheme a comparison is made with a method where the mesh of the fluid domain is adjusted to follow the motion of the fluid and the solid body. This is done at Stokes flow conditions, hence at $St = 0$ and $Re = 0$. The ME method as described by Equations (20)–(24) is used to couple the fluid to the solid domain. After each time step, the mesh is adjusted to maintain optimal element quality without changing the topology using Laplacian smoothing [11–14].

Figure 5 demonstrates the location of the leaflet using both a fixed mesh and a moving mesh. Figure 6 shows the tip displacement of the beam computed with both the 'updated-mesh' approach (solid line) and the 'fixed-mesh' approach (circles). The two methods produce almost identical results. However, for $t/T > 0.1$, the mesh updating procedure fails to produce a sufficiently good quality mesh and the computation subsequently breaks downs. In contrast, using the new method very large deflections of the beam can be achieved as is demonstrated in the next section.

6.2. Navier–Stokes flow

To demonstrate the capabilities of the FD/ME method using a fixed fluid domain, the motion of the beam is analysed at $St = 0.1$ and $Re = 100$. Figure 7 shows a sequence of computed flow

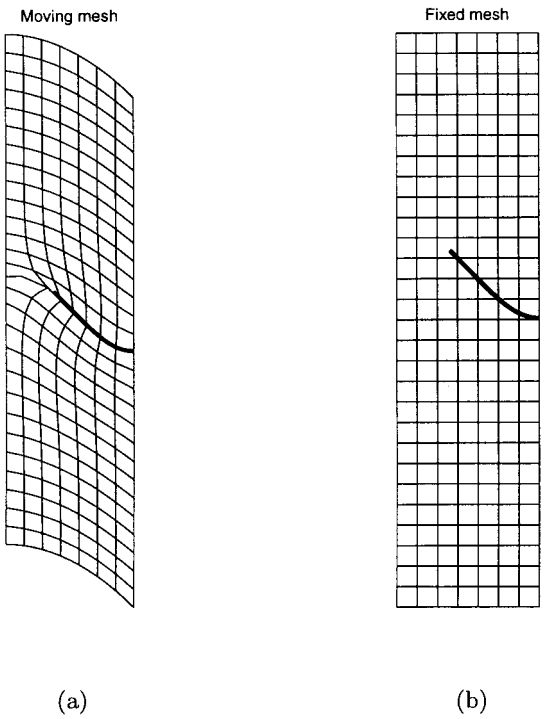

Figure 5. Position of leaflet using (a) a moving mesh or (b) a fixed mesh at $t/T = 0.1$.

fields and positions of the beam at increasing t/T ratio. Velocity vectors are shown at the mid-point nodes of the elements only for clarity of presentation.

The purpose of this example is to demonstrate some of the key features of the proposed method: it shows the analysis of large, complex, time-dependent motions of thin flexible bodies driven by viscous fluid forces, without the necessity of using complicated mesh updating algorithms as in the ALE method.

Starting at rest, during the first part of the cycle (a)–(e), the beam is pushed upward by the flow until the flow rate reaches its maximum. As soon as the flow rate starts to decrease (for $t/T > 0.25$), the elasticity causes the beam to bounce back, as can be clearly seen in (h)–(j). For $t/T > 0.5$ the flow reverses, accelerating the beam motion (k)–(n), to reach a fully deflected configuration when the flow rate reaches its maximum again. For $t/T > 0.9$, the above pattern repeats itself. This sequence of results clearly demonstrates the fluid–structure interaction capabilities of the FD/ME method.

A thinner beam, having wall thickness $0.0161H$, has also been analysed. This corresponds to a 24 per cent reduction in wall thickness. In particular, the behaviour during reversal of the flow rate is distinctly different form the thicker beam, as may be observed in Figure 8. This example illustrates the feasibility of the current method to investigate the impact of structural

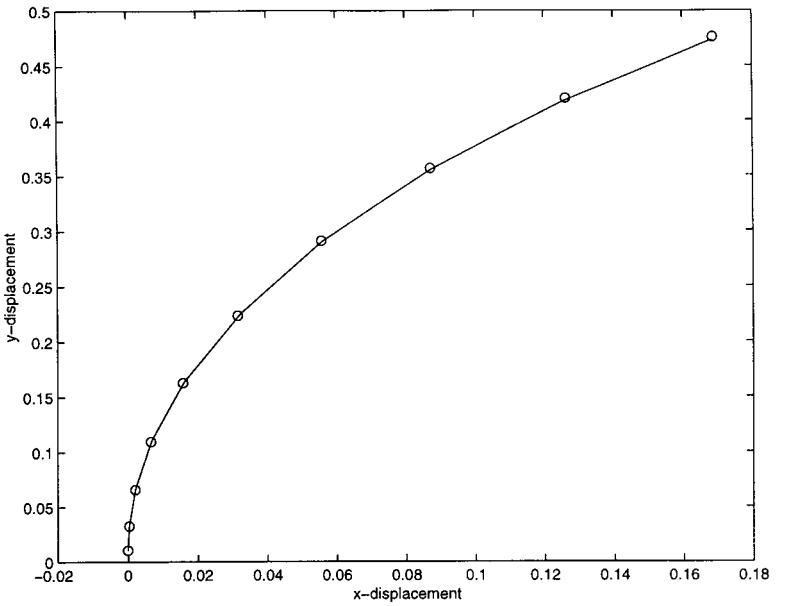

Figure 6. Comparison of the tip displacement using the moving and the fixed mesh approach. The solid line represents the result based on the moving mesh, and the circles represent the displacement of the tip while using a fixed mesh.

changes on fluid–structure interaction. It also demonstrates that due to the presence of viscous forces the snap-through behaviour of the beam, as present in Figure 8(c)–(f), can easily be handled by the current formulation without having to introduce path-following algorithms.

7. CONCLUSIONS

A new method to compute the fluid–structure interaction is introduced. It combines features of the FD method proposed by Glowinski *et al.* [4] and the ME method of Maday *et al.* [6]. It appears to be particularly suited for the analysis of the interaction of slender bodies with a fluid or gas. The method is based on the enforcement of continuity of motion along an arbitrary interface using Lagrange multipliers. Care should be taken in selecting the discretization space of the Lagrange multipliers. The choice that is proposed in this work is to select a piecewise discontinuous interpolation of one order lower than the discretization of the velocity and displacement variables, and is chosen spatially coincident with the edges of the elements along the interface Γ of the solid domain. Further research is necessary to prove the stability of this choice, in particular in the case where the mesh size of the solid and fluid domain are largely different.

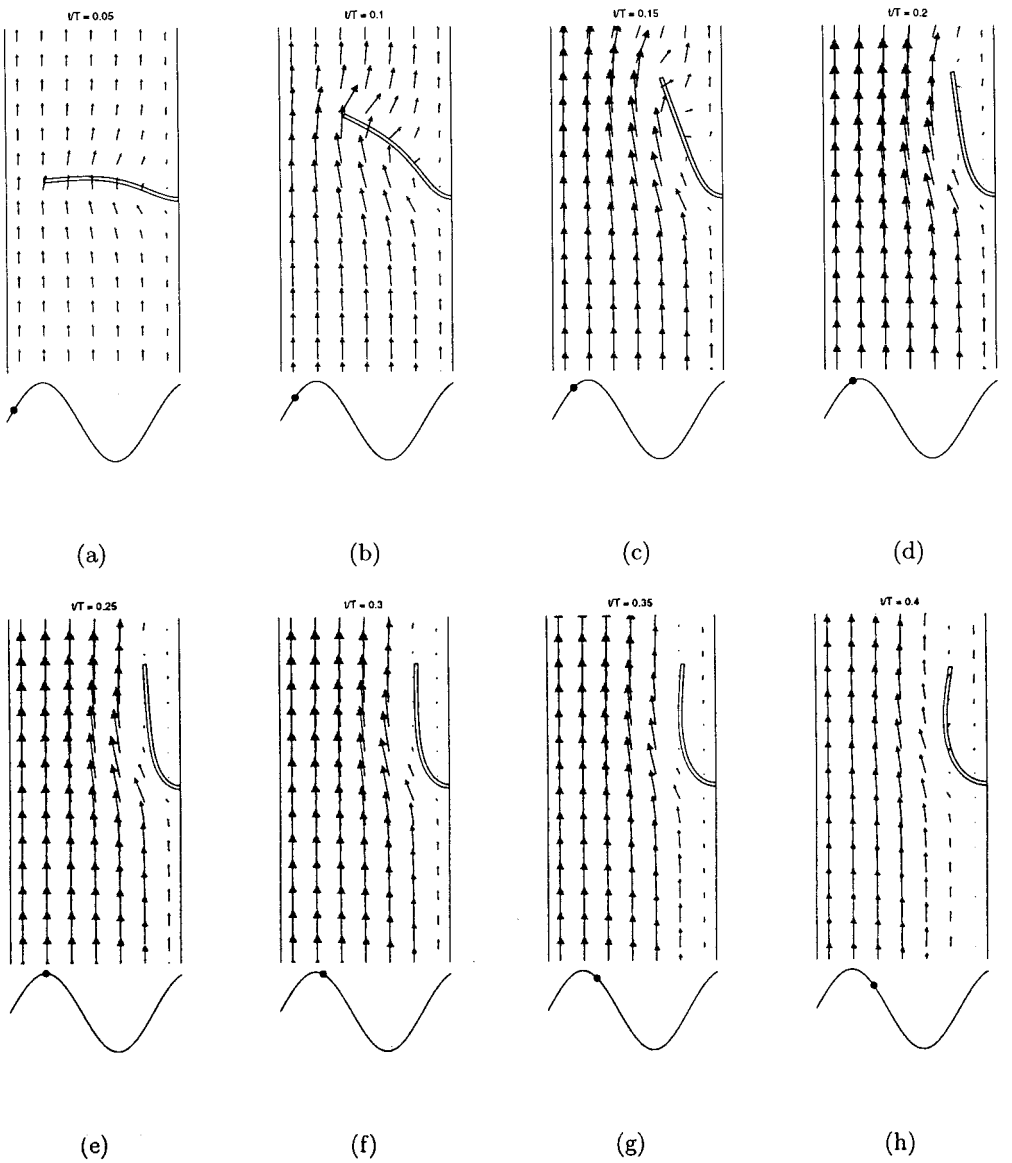

Figure 7. Motion of a beam, with wall thickness $0.0212H$, driven by pulsatile flow at $Sr = 0.1$ and $Re = 100$. Each picture also indicates the flow rate with respect to the cycle time.

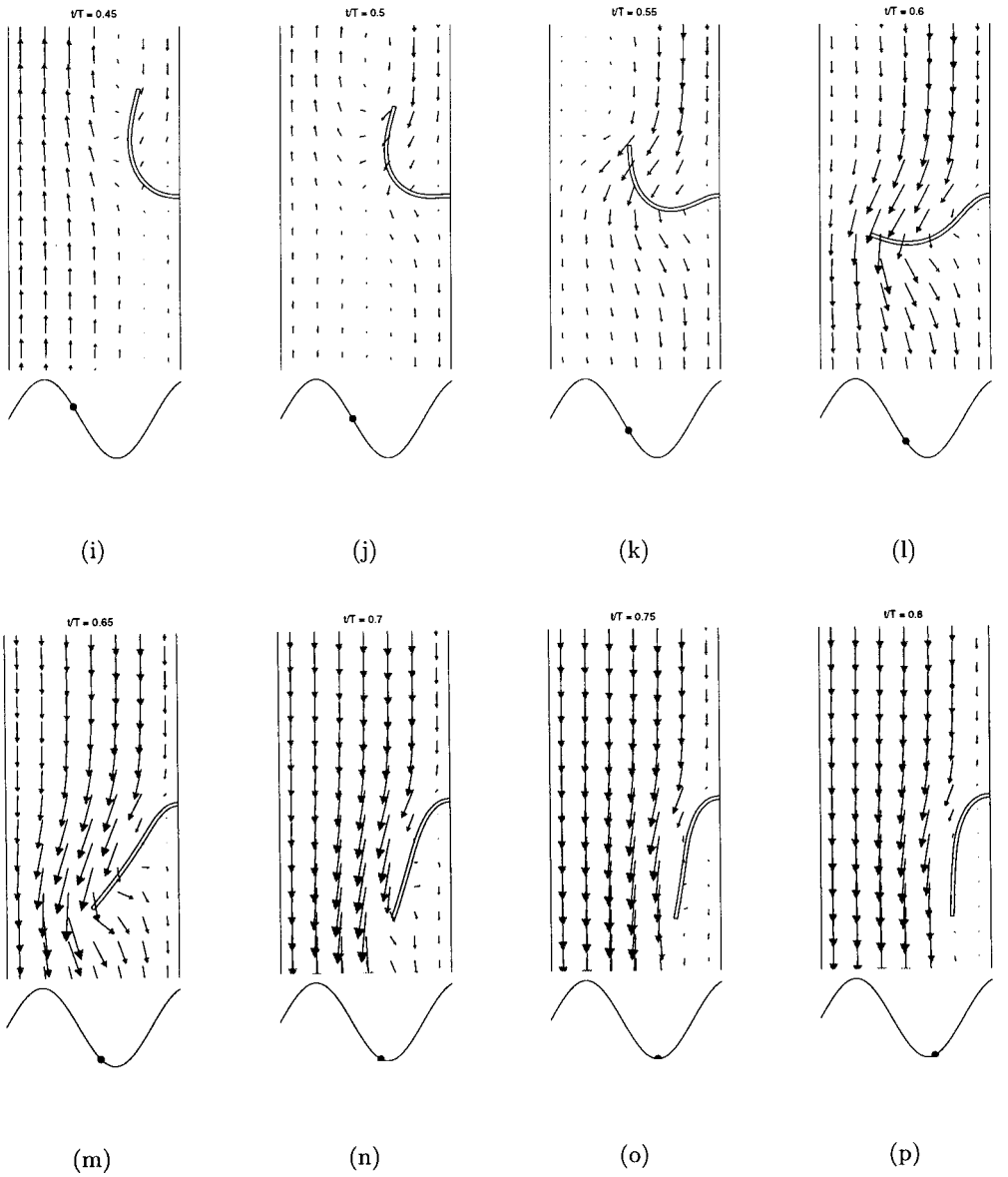

Figure 7 (*Continued*)

The key advantage of the proposed method compared with ALE-based methods is that the FD/ME method does not require any updating of mesh of the fluid domain, although it can easily be combined with ALE techniques. This makes the FD/ME method particularly

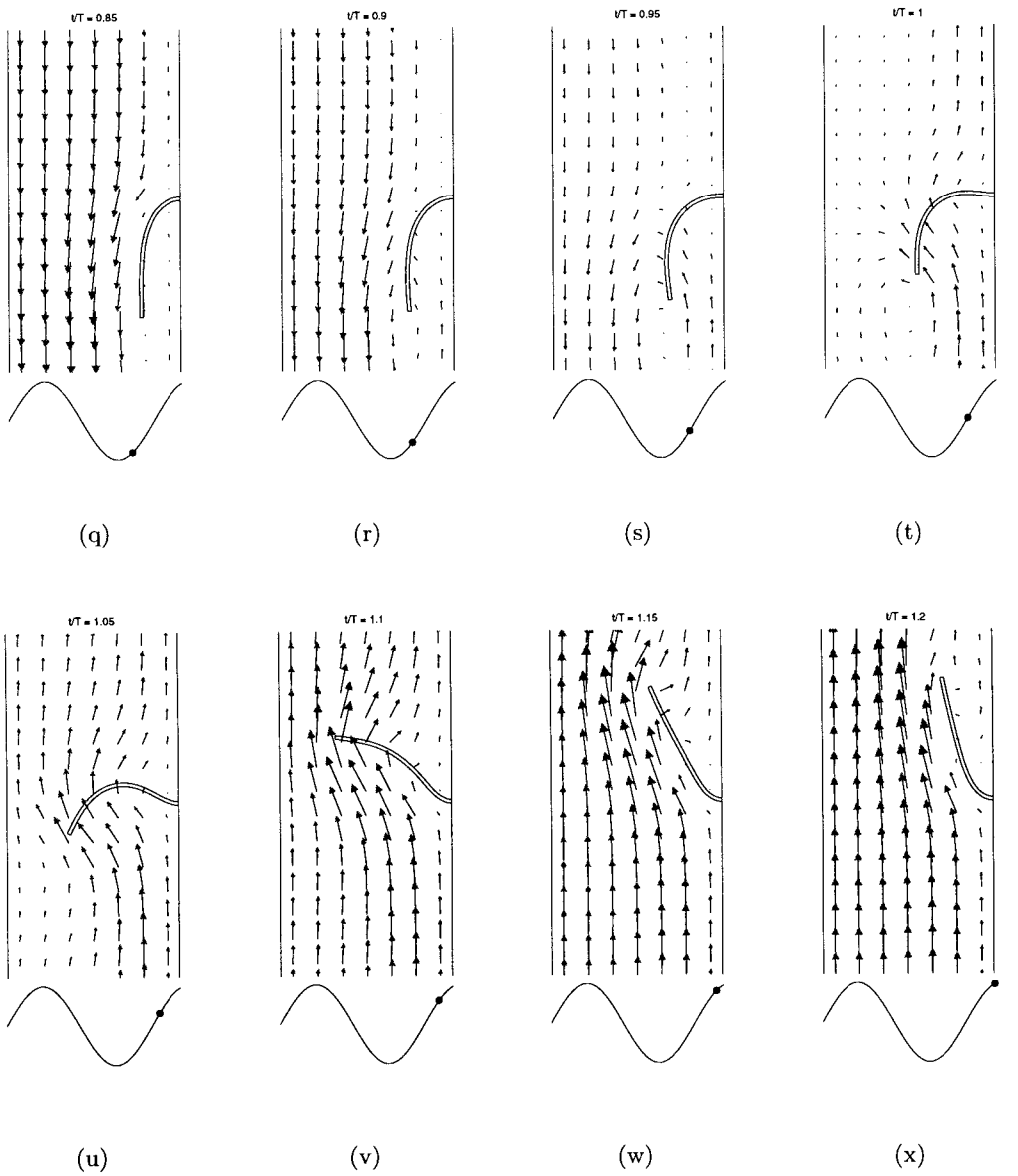

Figure 7 (*Continued*)

attractive for three-dimensional calculations, where a robust updating of the mesh to follow the motion of thin shell-like structures poses major difficulties.

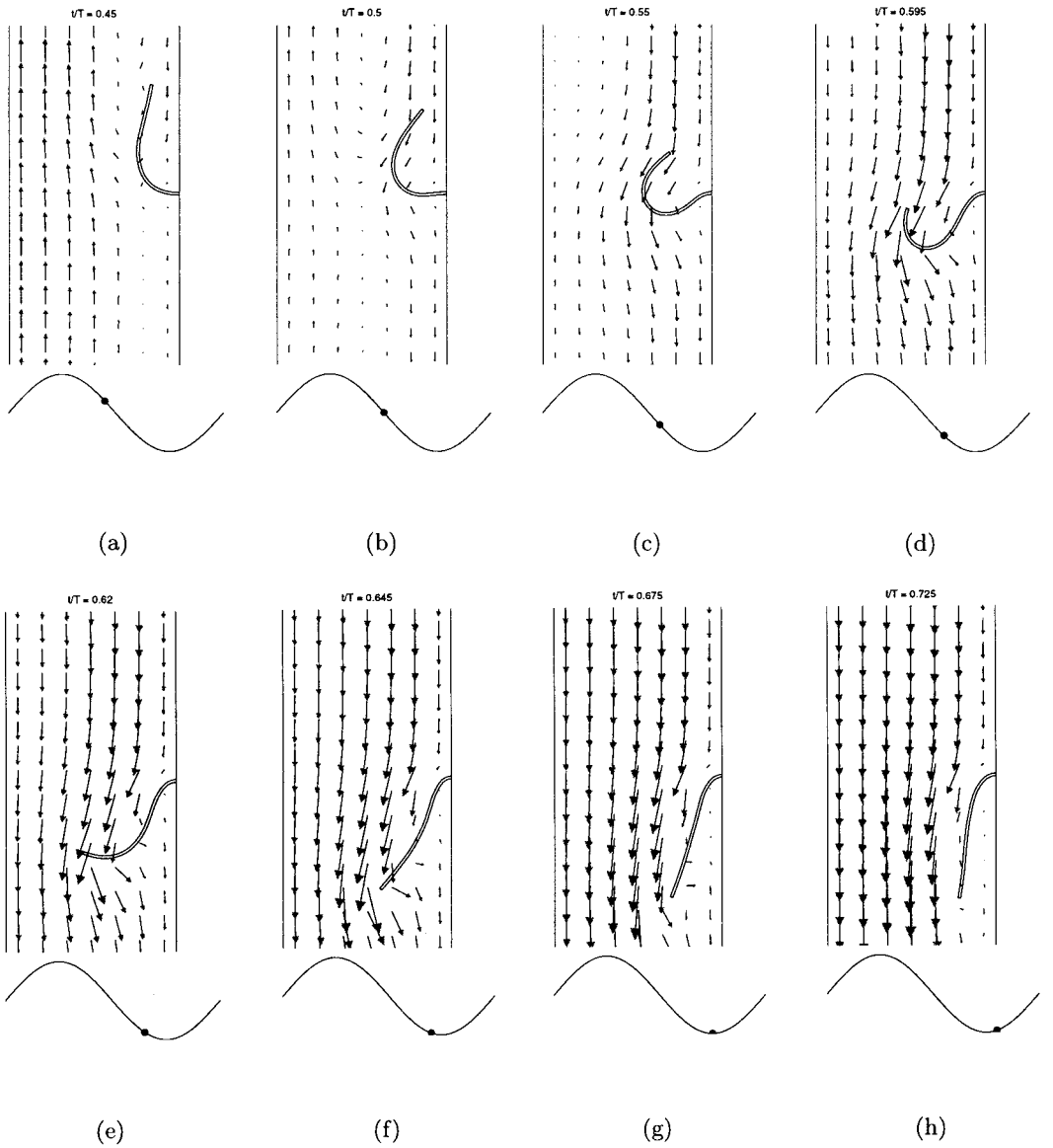

Figure 8. Motion of a beam, with wall thickness $0.0161H$, driven by pulsatile flow at $Sr = 0.1$ and $Re = 100$. Each picture also indicates the flow rate with respect to the cycle time.

The method has been demonstrated for both the Navier–Stokes case and the Stokes limit, where the fluid is assumed to be purely viscous. Extension to shear thinning fluids is expected to be straightforward, but application to viscoelastic fluids [15] is expected to be more complicated.

APPENDIX A. INFINITESIMAL STRAIN ELASTICITY PROBLEM

To derive the Lagrange multiplier formulation as represented by Equations (20)–(24) it is instructive to consider the infinitesimal strain limit for a linear elastic problem. In this case, neglecting inertia forces and volume forces, the momentum equation reduces to

$$\vec{\nabla}\cdot\boldsymbol{\sigma} = \vec{0} \tag{28}$$

The constitutive model is given by

$$\boldsymbol{\sigma} = {}^4\boldsymbol{C}\colon\ \boldsymbol{\varepsilon} \tag{29}$$

with ${}^4C$ a fourth-order elasticity tensor and $\boldsymbol{\varepsilon}$ the infinitesimal strain tensor

$$\boldsymbol{\varepsilon} = \frac{1}{2}(\vec{\nabla}\vec{d} + (\vec{\nabla}\vec{d})^T) \tag{30}$$

with $\vec{d}$ the displacement field. This set of equations must be supplemented with appropriate boundary conditions. Either the displacement field is prescribed along Γ_u or the external load vector $\vec{h}$ is prescribed along Γ_p with

$$\boldsymbol{\sigma}\cdot\vec{n} = \vec{h} \tag{31}$$

To simplify the notation it is assumed that $\vec{h} = \vec{0}$ in the sequel.

Consider two bodies, Ω_a and Ω_b, where along an interface Γ the displacements of the two bodies should be equal

$$\vec{d}_a - \vec{d}_b = \vec{0} \quad \text{along } \Gamma \tag{32}$$

The weak form of the equilibrium equations of each of the individual bodies without accounting for the interface constraint equation (32) may be derived from the minimization of the energy functional $I(\vec{v})$ defined by

$$I_\alpha(\vec{v}_\alpha) = \frac{1}{2}(\boldsymbol{\varepsilon}(\vec{v}_\alpha), {}^4\boldsymbol{C}\colon\ \boldsymbol{\varepsilon}(\vec{v}_\alpha))_\alpha, \quad \text{for } \alpha = a, b \tag{33}$$

where $(\,.\,,\,.\,)_\alpha$ denotes the inner product on the domain Ω_α, $\alpha = a, b$. The displacement constraint equation (32) may be imposed by means of Lagrange multipliers by defining the Lagrangian

$$L(\vec{v}_a, \vec{v}_b, \vec{\gamma}) = I_a(\vec{v}_a) + I_b(\vec{v}_b) + \int_\Gamma \vec{\lambda}\cdot(\vec{v}_a - \vec{v}_b)\,\mathrm{d}\Gamma \tag{34}$$

Requiring stationarity of the Lagrangian with respect to $\vec{v}_a$, $\vec{v}_b$ and the Lagrange multiplier, giving the associated solution fields $\vec{d}_a$, $\vec{d}_b$ and $\vec{\gamma}$, yields

$$(\boldsymbol{\varepsilon}(\vec{v}_a)\colon {}^4\boldsymbol{C}\colon \boldsymbol{\varepsilon}(\vec{d}_a))_a + \int_\Gamma \vec{\gamma}\cdot\vec{v}_a \, \mathrm{d}\Gamma = 0 \tag{35}$$

$$(\boldsymbol{\varepsilon}(\vec{v}_b)\colon {}^4\boldsymbol{C}\colon \boldsymbol{\varepsilon}(\vec{d}_b))_b - \int_\Gamma \vec{\gamma}\cdot\vec{v}_b \, \mathrm{d}\Gamma = 0 \tag{36}$$

$$\int_\Gamma \vec{\lambda}\cdot(\vec{d}_a - \vec{d}_b) \, \mathrm{d}\Gamma = 0 \tag{37}$$

This result may be generalized to give Equations (20)–(24).

REFERENCES

1. de Hart J, Cacciola G, Schreurs PJG, Peters GWM. A three-dimensional analysis of a fibre-reinforced aortic valve prosthesis. *Journal of Biomechanics* 1998; **31**: 629–638.
2. Cacciola G, Peters GWM, Baaijens FPT. A synthetic fiber reinforced stentless heart valve. *Journal of Biomechanics* 2000; **33**: 653–658.
3. Donea J, Giuliani S, Halleux JP. An arbitrairy Lagrangian–Eulerian finite element method for transient dynamic fluid–structure interactions. *Compter Methods in Applied Mechanics and Engineering* 1982; **33**: 689–723.
4. Glowinski R, Pan T-W, Periaux J. A fictitious domain method for Dirichlet problem and applications. *Computer Methods in Applied Mechanics and Engineering* 1994; **111**: 283–303.
5. Bernardi C, Maday Y, Patera AT. Domain decomposition by the mortar element method. In *Asymptotic and Numerical Methods for PDEs with Critical Parameters. NATO ASI Series C: Mathematical and Physical Sciences, Vol. 384*, Kaper HG, Garbey M (eds). Kluwer: Dordrecht, 1993; 169–186.
6. Ben Belgacem F, Maday Y. The mortar finite element method for three dimensional finite elements. *RAIRO Analyse Numerique* 1997; **31**: 289–302.
7. Peskin CS, McQueen DM. A three-dimensional computational method for blood flow in the heart: 1. Immersed elastic fibers in a viscous compressible fluid. *Journal of Computational Physics* 1989; **81**: 372–405.
8. Leveque RJ, Li Z. The immersed interface method for elliptic equations with discontinuous coefficients and singular sources. *SIAM Journal of Numerical Analysis* 1994; **31**: 1019–1044.
9. Bertrand F, Tanguy PA, Thibault F. A three-dimensional fictitious domain method for incompressible fluid flow problems. *International Journal for Numerical Methods in Fluids* 1997; **25**: 719–736.
10. Schwab C. hp-fem for fluid flow simulation. In *Lecture Notes of the Von Karman Institute for Fluid Dynamics, Higher Order Discretization Methods in Computational Fluids Dynamics*, 1998.
11. Winslow AM. Numerical solution of the quasilinear Poisson equation in a nonuniform triangle mesh. *Journal of Computational Physics* 1966; **1**(2): 149–172.
12. Field DA. Laplacian smoothing and Delaunay triangulations. *Communications in Applied Numerical Methods* 1988; **4**: 709–712.
13. Hansbo P. Generalized Laplacian smoothing of unstructured grids. *Communications in Numercal Methods in Engineering* 1995; **11**: 455–464.
14. van Rens BJE, Brokken D, Brekelmans WAM, Baaijens FPT. A 2-dimensional paving mesh generator for triangles with controllable aspect ratio and quadrilaterals with high quality. *Engineering with Computers* 1998; **14**: 248–259.
15. Baaijens FPT. Mixed finite element methods for viscoelastic flow analysis: a review. *Journal of Non-Newtonian Fluid Mechanics* 1998; **79**: 361–385.

